

 Open access • Posted Content • DOI:10.20944/PREPRINTS201812.0325.V1

Energy Efficient Tri-State CNFET Ternary Logic Gates — [Source link](#)

[Sepehr Tabrizchi](#), [Fazel Sharifi](#), [Abdel-Hameed A. Badawy](#)

Published on: 28 Dec 2018 - [arXiv: Emerging Technologies](#)

Topics: [Logic gate](#), [Electronic circuit](#), [Transistor](#), [State \(computer science\)](#) and [Ternary operation](#)

Related papers:

- [Enabling energy-efficient ternary logic gates using CNFETs](#)
- [Design of energy-efficient and robust ternary circuits for nanotechnology](#)
- [Design Methodologies for Ternary Logic Circuits](#)
- [An Efficient Design Methodology for CNFET Based Ternary Logic Circuits](#)
- [Design of ternary logic gates and circuits using GNFETs](#)

Share this paper:    

View more about this paper here: <https://typeset.io/papers/energy-efficient-tri-state-cnfet-ternary-logic-gates-hdt2utrfd7>

1 Article

2 Energy Efficient Tri-State CNFET Ternary Logic 3 Gates

4 Sepher Tabrizchi ¹, Fazel Sharifi ² and Abdel-Hameed A. Badawy ^{3,*}

5 ¹ School of Computer Science Institute for Research in Fundamental Sciences (IPM), Tehran, Iran;
6 s.tabrizchi@ipm.ir

7 ² Department of Electrical and Computer Engineering, Graduate University of Advanced Technology,
8 Kerman, Iran; f.sharifi@kgut.ac.ir

9 ³ Klipsch School of Electrical and computer Engineering, New Mexico State University, Las Cruces, NM,
10 USA, and has a joint appointment with the Los Alamos National Laboratory, Los Alamos, NM;
11 badawy@nmsu.edu

12 * Correspondence: badawy@nmsu.edu; Tel.: +1-575-646-6476

13

14 **Abstract:** Traditional silicon binary circuits continue to face challenges such as high leakage power
15 dissipation and large area of interconnections. Multiple-Valued Logic (MVL) and nano-devices are
16 two feasible solutions to overcome these problems. In this paper, we present a novel method to
17 design ternary logic circuits based on Carbon Nanotube Field Effect Transistors (CNFETs). The
18 proposed designs use the unique properties of CNFETs, e.g., adjusting the Carbon
19 Nanotube (CNT) diameters to have the desired threshold voltage and have the same mobility of P-
20 FET and N-FET transistors. Each of our designed logic circuits implements a logic function and its
21 complementary via a control signal. Also, these circuits have a high impedance state which saves
22 power while the circuits are not in use. We show a more detailed application of our approach by
23 designing a two-digit adder-subtractor circuit. We simulate the proposed ternary circuits using
24 HSPICE via standard 32nm CNFET technology. The simulation results indicate the correct
25 operation of the designs under different process, voltage and temperature (PVT) variations.
26 Moreover, we designed a two-digit adder/subtractor and a power efficient ternary logic ALU based
27 on the proposed gates. Simulation results show that the two-digit adder/subtractor using our
28 proposed gates has 12X and 5X lower power consumption and PDP (power delay product)
29 respectively, compared to previous designs.

30 **Keywords:** Multiple Valued Logic (MVL); CNFET; Energy-Efficiency; Nano-electronics; Ternary
31 Logic, Adder, ALU

32

33 1. Introduction

34 Conventional silicon binary computing faces significant problems in terms of power and
35 performance. Some of the most important challenges are the severe short channel effects of the Si-
36 MOSFET and the restriction in the number of wires and pins of the chips that play more important
37 roles than the device geometry. To overcome these challenges, one solution is to utilize non-silicon
38 and non-binary circuits [1].

39 In order to use non-binary computing, the MVL paradigm has been introduced as an alternative
40 to binary computing. In MVL, more than two logic values are used for data representation. More
41 information can be conveyed over the same line and more data can be stored per memory cell by
42 utilizing MVL techniques [1]. Also, using more than two significant logic levels leads to fewer
43 computational steps, potentially fewer gates and considerable reduction in the number of
44 interconnections and pins [2-4]. It was proven that e base ($e \approx 2.718$) leads to the most efficient
45 implementation of the switching systems among all MVL systems [2]. Therefore, ternary logic is
46 superior to binary logic since three is the closest integer to e. Ternary logic provides the most

47 efficiency with its lower energy consumption, as a result of the reduction in the number of
48 interconnection wires and the cost of data movement.

49 In nanoscale CMOS devices leakage power is an important part of its total energy consumption.
50 Other critical challenges are the reduced gate control and velocity saturation [5]. Therefore, to
51 continue the historical improvement in chip transistor count, density and performance while
52 operating at low-power, some emerging devices and technologies have attracted considerable
53 attention in the recent years as alternatives for CMOS, such as quantum dot cellular automata (QCA),
54 carbon nanotube field effect transistor (CNFET), single electron transistor (SET), nano magnetic
55 devices, *etc.* [6-8]. Among these new technologies, CNFETs have attracted a lot of attention as a
56 potential successor for CMOS because of its outstanding characteristics such as similarities with
57 MOSFET, high carrier mobility, high I_{ON}/I_{OFF} ratio, unique one dimensional band structure and near
58 ballistic transportation [9, 10].

59 CNFET transistors are even more interesting, when they are used in designing MVL circuits.
60 MVL circuit design is based on multiple threshold design techniques and adjusting the threshold
61 voltage of CNFETs is easily possible by changing the diameter of the nanotubes [11,12]. In recent
62 years, some MOSFET and CNFET MVL circuits, have been presented for ternary and quaternary logic
63 [10,11,13-21]. However, they have some critical drawbacks such as using very large ohmic resistors
64 [13,14], requiring obsolete depletion-mode MOSFET [15,17-20], non-full swing nodes and limited fan-
65 out [21]. In this paper, we propose a novel method for designing ternary logic gates Buffer/NOT,
66 AND/NAND, and OR/NOR. Each of the designs produces a logic function with its complimentary
67 by a control signal. Moreover, a third state of high impedance is introduced to achieve power
68 efficiency if none of the two possible gates is needed.

69 This paper extends the contributions of [22], in which ternary basic gates based on CNTFETs
70 were introduced. In this current paper, we make additional contributions by presenting a two-digit
71 adder/subtractor as an application for the proposed basic gates in addition to detailed analysis with
72 several figures of merit, such as propagation delay, power dissipation and the power-delay product
73 (PDP). In addition, a low power ternary arithmetic logic unit (ALU) based on the presented circuits
74 is designed and analyzed.

75 The rest of this article is organized as follows: Section II briefly reviews some background on
76 CNFET devices and ternary logic. Section III describes the proposed designs. Section IV presents the
77 simulation results and analyses. Finally, section V concludes the article.

78 2. Background

79 2.1 Carbon Nanotube Field Effect Transistor

80 A carbon nanotube (CNT) is a sheet of graphene rolled up along a chirality vector [23]. The
81 chirality vector of a CNT is defined by (n, m) pair. If $n-m = 3k$ ($k \in \mathbb{Z}$) where \mathbb{Z} is the set of integer
82 numbers, then the CNT behaves like a metal, otherwise like a semiconductor [12].

83 Metallic nanotubes are attractive as future interconnects because of their superior properties,
84 such as large current carrying capacity, and high thermal conductivity [24]. Also semiconducting
85 nanotubes have great advantages. They can be used as channels in field effect transistors. They have
86 high charge carrier mobility, lower sub-threshold swing and fewer parasitic elements [3]. Moreover,
87 they are very attractive to the Silicon semiconductor industry for the following reasons:

88 (1) The operation principle and the device structure are similar to CMOS devices; therefore, we can
89 reuse the CMOS fabrication process and established CMOS design infrastructure. (2) CNFETs show
90 significant improvements in device performance metrics such as delay and power consumption in
91 experimental results [25].

92 This three (or four) terminal device (CNFET) is turned on or off electrostatically via the gate and
93 its threshold voltage (V_{th}). One of the most effective properties of CNFET, which makes it very
94 suitable for designing digital circuits, is that the desired threshold voltage can be obtained by
95 choosing the proper diameter for the CNT. The threshold voltage of a CNFET is given by the
96 following equations, where, e is the unit electron charge, E_{bg} is the CNT bandgap, a_0 (≈ 0.142 nm) is

97 the carbon to carbon bond length in a CNT and V_π (≈ 3.033 eV) is the carbon π - π bond energy in the
 98 tight bonding model [26].

99

(1)

$$V_{th} \approx \frac{E_{bg}}{2e} = \frac{a_0 E_\pi}{e D_{CNT}} \approx \frac{0.436}{D_{CNT} \text{ (nm)}} \quad (1)$$

$$D_{CNT} = \frac{\sqrt{3} a_0 \sqrt{n^2 + m^2 + nm}}{\pi} \approx 0.0783 \sqrt{n^2 + m^2 + nm} \quad (2)$$

100

101

102 According to Equation (2), the threshold voltage of a CNFET is inversely proportional to the
 103 CNT diameter.

104

105 Although CNFETs are promising, there are several challenges that need to be addressed. There
 106 are some difficulties for synthesis or growth of nanotubes with identical diameters and chiralities.
 107 Changes in tubes' diameter and wrapping angle, defined by the chirality indices (n, m), will shift the
 108 electrical conductivity and CNFET threshold voltage. However, many effective and feasible solutions
 109 have already been presented in the literature for growing CNTs with a specific chirality and setting
 110 the desired threshold voltage [27, 28]. Moreover, it is difficult to control the exact placement and
 111 alignment of CNTs at a VLSI scale. Mispositioned CNTs may cause incorrect logic functionality
 [29,30].

112 2.2. Ternary Logic

113 Ternary logic consists of three significant logic levels represented by "0", "1" and "2" symbols.
 114 These logic levels are commonly counterpart to Zero Volts, $\frac{1}{2}V_{DD}$ and V_{DD} voltage levels, respectively.
 115 The ternary basic logic operations, which are the building blocks of many other complex logical and
 116 arithmetic quaternary circuits, can be defined according to (3), (4) and (5).

117

$$X_i, X_j \in \{0, 1, 2\}$$

$$X_i + X_j = \text{Max} \{X_i, X_j\} \quad (3)$$

$$X_i \cdot X_j = \text{Min} \{X_i, X_j\} \quad (4)$$

$$\overline{X_i} = 2 - X_i \quad (5)$$

118

119 where, $-$ denotes the arithmetic subtraction, the operations $+$, \cdot , and $\overline{\quad}$ are the OR, AND, and
 120 NOT in ternary logic, respectively [31].

121 Three different type of ternary gates can be designed for each function. As an example for
 122 ternary inverter three logic gates can be defined; Standard Ternary Inverter (STI), Positive Ternary
 123 Inverter (PTI), and Negative Ternary Inverter (NTI). The truth tables of these gates for ternary
 124 inverter are shown in Table 1.

125

Table 1. Truth Table of PTI, NTI and STI, where a is the input

a	PTI(a)	NTI(a)	STI(a)
0	2	2	2
1	2	0	1
2	0	0	0

126

127

128 2.3. Related Works

129 There exists in the literature state-of-the-art CNFET-based ternary circuits. Raychowdhury and
130 Roy introduced a CNFET-based ternary design [1]. The design had large resistive loads. This is hard
131 to implement and integrate with CNFETs and also causes performance degradation and wastes area
132 and power. Another ternary design has been presented by Lin, Kim, and Lombardi [12]. They
133 replaced the resistors used in [1] with P-CNFET active loads which led to less area overhead, larger
134 noise margins and higher performance compared to the previous design.

135 Moaiyeri *et al.* [32] presented ternary logic circuits based on the complementary CNFET design
136 style which uses three different threshold voltages. This design produces NTI, PTI and STI by a single
137 circuit unlike previous designs. We adopt the design style of [32] throughout this paper.

138 3. Proposed design(s)

139 In this section, we introduce ternary logic gates, including ternary Buffer/NOT, ternary
140 AND/NAND and ternary OR/NOR gates. The proposed designs use just two different diameters for
141 their CNFETs. From Equations (1) and (2), the CNFETs should have 0.783 and 1.487 nm diameters,
142 respectively. The chiral numbers should be (10, 0) and (19, 0), respectively. The threshold voltages
143 ($|V_{th}|$) should be 0.557V and 0.293V, respectively. Moreover, in these designs we can produce a high
144 impedance state, which is useful when any of the logic functions is not needed. This state consumes
145 very lower power compared to the two other states which have static power dissipation. In summary,
146 in this paper we propose a ternary family of logic circuits which can have three output states specified
147 via a control signal.

148 3.1. Ternary Buffer/Inverter

149 The proposed ternary Buffer/NOT circuit is shown in Fig.1. This circuit can act as a buffer or an
150 inverter for a ternary input using a control signal (S).

151 When the signal $S = 0$, the circuit acts as a ternary buffer. In this case, if $IN = 0$, both NTI and PTI
152 nodes (shown in Fig. 1) will be V_{DD} , T5, T6 will be OFF and T3 and T4 will be ON, consequently, the
153 output will be discharged to the ground through path 4. When $IN = 2$ (V_{DD}) the NTI and PTI nodes
154 will be 0, and T1 and T2 will be ON and the output will charge to V_{DD} (path 3). When, $IN = 1$ ($\frac{1}{2}V_{DD}$),
155 PTI and NTI are V_{DD} and 0 respectively and T1, T2, T3 and T4 will be ON. So with a resistive voltage
156 division, the output will be $\frac{1}{2}V_{DD}$.

157 When $S = 2$ (V_{DD}), the circuit performs the NOT function. In this case, T1 and T2 are OFF and T5
158 and T6 are ON. Assume that $IN=0$, so STI and PTI will be V_{DD} and consequently the output will be
159 V_{DD} through paths 1 and 2. For other inputs the output will be determined based on a resistive
160 division.

161 Finally, when $S=1$ ($\frac{1}{2}V_{DD}$), the output will be high impedance (HiZ). In this case, T1, T4, T5 and
162 T6 will be OFF because of their threshold voltages which are higher than $\frac{1}{2}V_{DD}$. Therefore, we do not
163 have any path to the output. In this state, the circuit consumes very low power compared to the other
164 states which consume static power. This state of the circuit is very useful in low power applications
165 where no need for neither the buffer nor the inverter functionality continuously. The operation of this
166 design is summarized in Table 2.

167 Figures 2 and 3 show the voltage transfer characteristic (VTC) curves of the presented ternary
168 buffer and inverter receptively. These schematics verify the correct operation and steep curve in the
169 transition region, which leads to low average static power consumption. We used PTI(s) and NTI(s)
170 for controlling T4 and T5 to have lower OFF current and consequently lower power consumption.

171 3.2. Ternary AND/NAND – OR/NOR

172 Using the same design methodology for the ternary Buffer/NOT circuit, we design a new ternary
173 AND/NAND and a new ternary OR/NOR. The operation principles of these two circuits are similar
174 to the ternary Buffer/NOT gate.

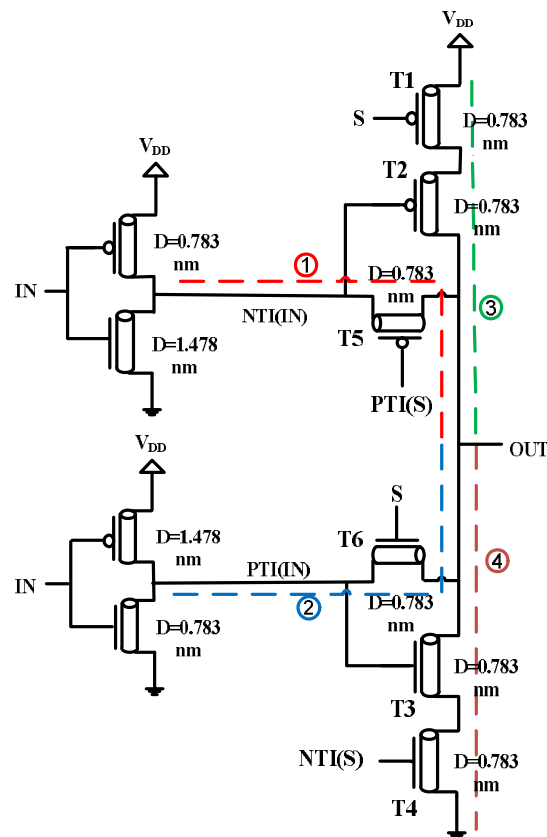
175

176

177

Table 2. Truth Table for the operation of the Buffer/NOT gate

S	IN	OUT
0	0	0
0	1	1
0	2	2
1	0	HiZ
1	1	HiZ
1	2	HiZ
2	0	2
2	1	1
2	2	0



178

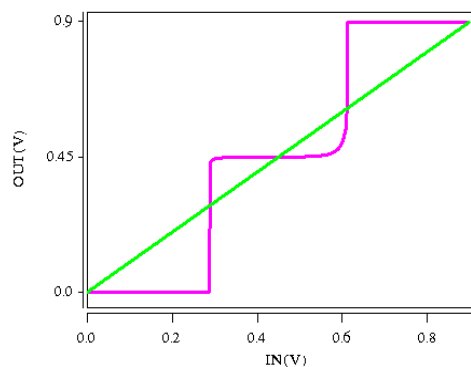
179

180

181

Figure 1. The circuit design of our ternary Buffer/NOT Gate. This circuit has four different paths from V_{DD} and ground to the output which are represented by numbers 1 – 4. For each of the different inputs two or three paths will be active.

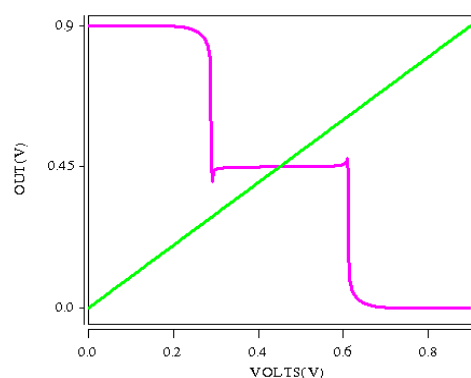
182



183
184

185 **Figure 2.** The Voltage Transfer Characteristic (VTC) of our proposed ternary Buffer

186



187
188

189 **Figure 3.** The Voltage Transfer Characteristic (VTC) of our proposed ternary Inverter

190 The schematics of the proposed AND/NAND and OR/NOR circuits are shown in Figs. 4 and 5,
191 respectively. The operation of the ternary AND/NAND can be summarized as follows:

192 When both inputs (IN1, IN2) are around V_{DD} and $S = 0$, NTNAND and PTNAND nodes are
193 discharged to ground, so the output will be V_{DD} through path 3. While one of the inputs is around
194 $\frac{1}{2}V_{DD}$ and the other one is equal to or greater than $\frac{1}{2}V_{DD}$, both paths 3 and 4 are activated and the
195 output will be $\frac{1}{2}V_{DD}$. Moreover, when one or both of the inputs is around 0, both T3 and T4 are ON
196 and the other paths to the output are disconnected, consequently the output is 0. In case of $S = 2$, T1
197 and T4 are OFF and the circuit implements the NAND functionality. During these operating
198 conditions, the output will be determined based on paths 1 and 2. Finally, if $S = 1$ ($\frac{1}{2}V_{DD}$), all paths
199 through the output will be disconnected and the output is HiZ. The principle operation of the
200 proposed ternary OR/NOR is very similar to the AND/NAND circuit operation.

201 The proposed circuits utilize CNFETs with only two different diameters for their CNTs, while
202 most of the designs of ternary logic gates in the literature need at least three distinct diameters. This
203 property improves robustness to process variation and enhances the manufacturability of the
204 proposed circuits.

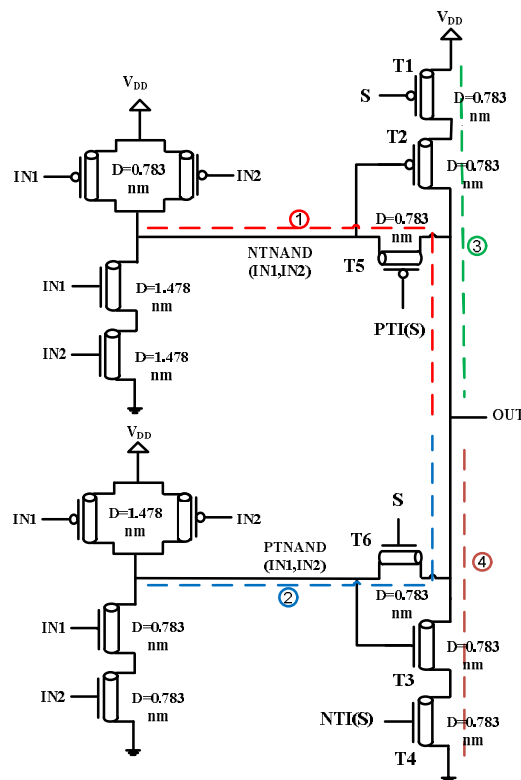
205 3.3. Two-Digit Ternary Adder/Subtractor

206 Multi-digit ternary adder/subtractor has been designed using the proposed Buffer/Inverter.
207 Figure 6 shows a two-digit adder/subtractor which can perform addition and subtraction by a selector
208 signal S. when $S=0$, the outputs of the binary buffer and the ternary Buffer/Inverter are zero and A
209 respectively, thus the circuit will add two digits. But, when $S=2$ (V_{DD}), the output of the binary buffer
210 and the ternary Buffer/Inverter are 1 ($\frac{1}{2}V_{DD}$) and \bar{A} respectively. Therefore, the circuit will perform

211 subtraction. The applied binary buffer gets values 0 and 2 and produces 0 and 1 respectively. By using
 212 the proposed ternary Buffer/Inverter we would save N multiplexers for N -digit adder/subtractor
 213 circuit.

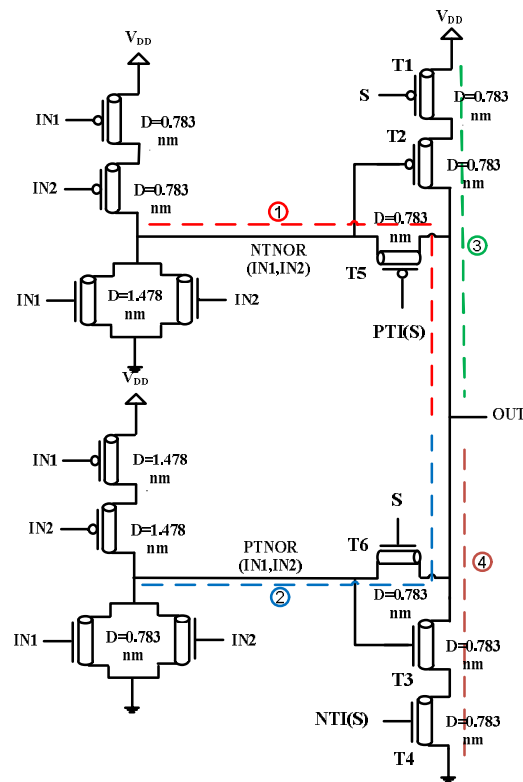
214 3.4. Ternary Arithmetic and Logic Unit (ALU)

215 In this section, we present two ternary arithmetic and logic units (ALUs). The proposed ALUs
 216 perform nine different logic and arithmetic operations. Table 3 shows the operations the ALUs.
 217 Figure 7 shows the first design which is based on multiplexers. The operations are controlled by two
 218 signals (S_0 and S_1) which are connected to the multiplexers selectors. When S_0 is 1, the ALU performs
 219 arithmetic operations (Addition, Subtraction and Increment), but when S_0 is 0 or 2, the ALU performs
 220 logic functions controlled by S_1 as shown in Table 3. This design is simple and modular but uses
 221 multiplexers which increases the transistor count, chip area, complexity and power consumption.



222

223 **Figure 4.** The circuit design of our proposed ternary AND/NAND. If $S = 0$, this circuit acts as an AND
 224 gate. If $S = 2$, it acts as a NAND gate, and if $S = 1$, the output is High Impedance (HZ).



225

226

227

Figure 5. The circuit design of our proposed ternary OR/NOR gate. If $S = 0$, this circuit acts as an OR gate. If $S = 2$, it acts as a NOR gate, and if $S = 1$, the output is High Impedance (HZ).

228

229

230

231

232

233

234

235

236

237

238

239

240

241

242

243

244

245

246

To decrease the number of transistors and take advantage of the proposed ternary logic gates, we present the second ALU design which is shown in Fig. 8. In this design, we have eliminated the multiplexers by using the third state (HiZ) of the ternary gates proposed in Section III.

Four customized circuits have been designed to produce additional control signals (C_1 , C_2 , C_3 and C_4) for ternary gates by using two main control signals (S_0 and S_1). These circuits are shown in Fig. 9 and the output of each circuit is in Table 3.

Table 3 summarizes the functionality of the proposed ternary ALU. As it is indicated in Table 3, when $S_0=1$, the output of the logic unit is HiZ and the ALU performs an arithmetic operation based on the value of S_1 . But, when $S_0=0$ or $S_0=2$, the output of the arithmetic unit will be HiZ by signal C_4 , and by adjusting a proper value for the S_1 signal a desired logic function will be performed. For example, when $S_0=0$ and $S_1=2$, the C_3 output will be zero and C_1 , C_2 , and C_4 are 1.

Thus, the outputs of the two first logic gates (Buffer/Inverter and AND/NAND) and the arithmetic circuit are HiZ and consequently the ALU output will produce OR(A, B).

The proposed ALUs can have more functions by adding more control signals. Also, having HiZ state in the proposed ternary gates has two main advantages in the second design. (1) We do not need to use multiplexers in the ALU design which reduces area, complexity, and power consumption. (2) We can eliminate static power dissipation and improve power efficiency in unused traditional ternary gates.

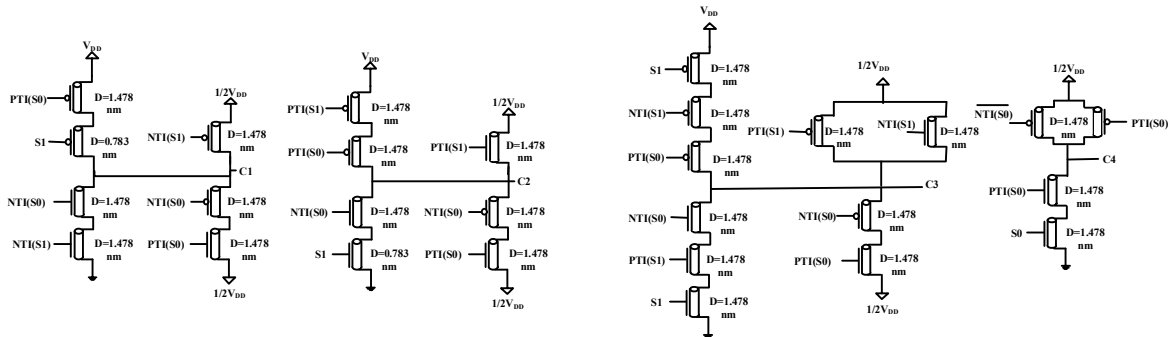
247

248

Table 3. The truth table detailing the Operations and functionality of the presented ternary ALU and its control signals

S_0	S_1	C_1	C_2	C_3	C_4	Logic Unit Output	Arith Unit Output	ALU Output
1	0	1	1	1	0	HZ	Add	Add
1	1	1	1	1	0	HZ	Increase	Increase
1	2	1	1	1	0	HZ	Subtract	Subtract
0	0	0	1	1	1	Buffer	HZ	Buffer

0	1	1	0	1	1	AND	HZ	AND
0	2	1	1	0	1	OR	HZ	OR
2	0	2	1	1	1	NOT	HZ	NOT
2	1	1	2	1	1	NAND	HZ	NAND
2	2	1	1	2	1	NOR	HZ	NOR



249
250
251

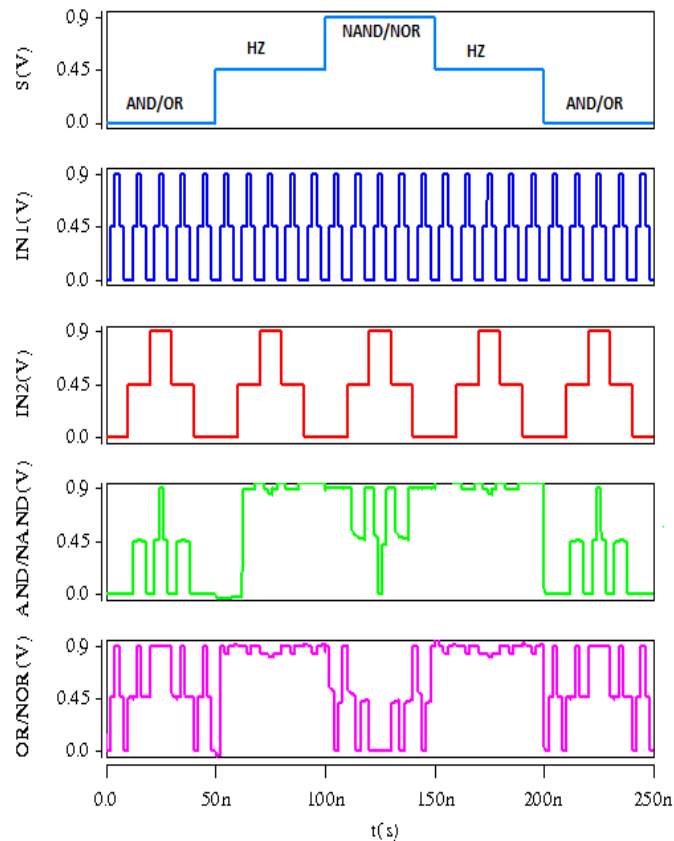
Figure 9. The Customized circuits to produce control signals using in the presented ALU. These circuits generate C1, C2, C3 and C4 signals which act as control signals for ternary basic gates in ALU.

252 4. Simulation Results

253 In this section, we present the simulation results of the proposed circuits. Simulations are
254 conducted using the HSPICE simulator for 32 nm technology with the Stanford Compact SPICE
255 model for CNFETs including the non-ideal and parasitic characteristics [33, 34]. Since this is the first
256 attempt to design ternary logic gates with three output states, we could not compare our designs
257 directly with state-of-the-art designs. Figure 10 shows the output waveforms of the presented circuits
258 which confirms the correct operation of the designs.

259 Table 4 provides the simulation results of the ternary designs including delay, average power
260 consumption and power delay product (PDP). As indicated in Table 4, the Buffer/NOT gate has the
261 lowest delay. But due to the higher power consumption, it has a higher PDP compared to
262 AND/NAND and OR/NOR designs. In order to have a fair comparison with previous ternary logic
263 gates, we have simulated two-digit ternary adder/subtractor using the proposed designs and
264 previous designs presented by Moaiyeri *et al.* [32], and the results are shown in Table 5. Based on the
265 results using the proposed designs, a two-digit adder/subtractor could save power consumption
266 more than 12X compared to Moaiyeri *et al.* [32]. Also, the PDP of the circuit using the proposed
267 designs is about 5X better than the design of Moaiyeri *et al.* [32].

268 Moreover, we do sensitivity analysis for our proposed ternary circuits under different conditions
269 and variations. We simulate the circuits with different temperatures from 0°C –



270

271

272

273

Figure 10. Output waveforms of the proposed ternary AND/NAND and OR/NOR gates. When $S = 0$, the circuits perform AND/OR functions. When $S = 1$, the output is high impedance. When $S = 2$, the circuits perform NAND/NOR operation.

274

Table 4. Delay, power and Power Delay Product (pdp) of our designed Circuits

Design	Delay (E-11s)	Maximum Delay (E-11s)	Power (E-7W)	PDP (E-17J)
Buffer	1.878	1.878	17.711	3.326
NOT	0.781	1.878	7.0485	1.946
AND	2.762	2.762	10.54	2.879
NAND	1.202	2.732	10.54	2.879
OR	2.732	2.732	10.54	2.879
NOR	1.314	2.732	10.54	2.879

275

276

277

Table 5. Simulation results of two-digit ternary Add/Sub using the proposed designs and designs [11]

Design	Maximum Delay (E-11s)	Power (E-7W)	PDP (E-17J)
two Digit Add/Sub Using proposed designs	13.80	47.57	65.64
two Digit Add/Sub Using designs [32]	5.79	617.2	357.3

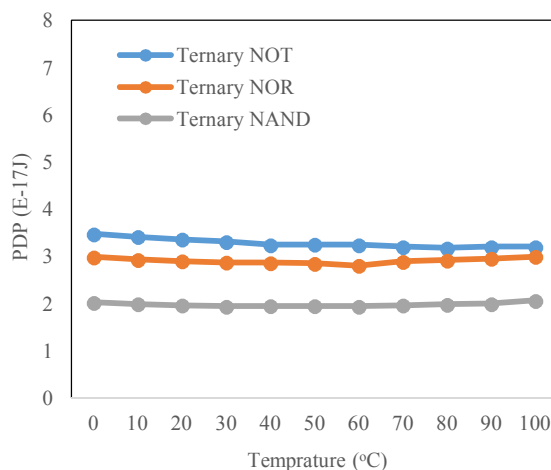
278

279

280

281

100°C. Figure 11 clearly shows that these designs have almost constant PDP for all temperatures due to the high thermal stability of CNFETs.

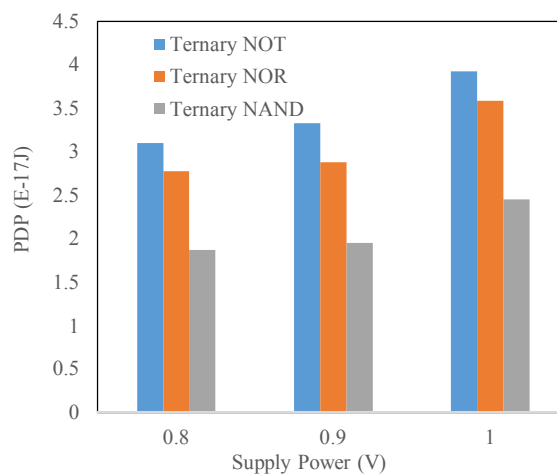


282

283

Figure 11. PDP variation against temperatures variation

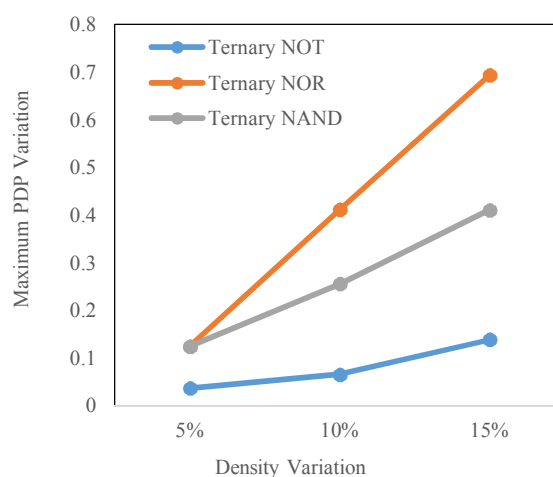
284



285

286

Figure 12. PDP variation in different supply voltages



287

288

289

290

Figure 13. Maximum PDP variation against CNTs density variation. Density includes the CNT's pitch and the number of CNTs under gate.

291

292

293

Figure 12 shows the PDP variation of the circuits under different supply voltages. Designs are simulated in 0.8, 0.9 and 1V and the proposed ternary NAND gate has lower PDP because of its lower power consumption under all supply voltages.

294 The operation of the ternary gates is also examined in the presence of process variation. One of
 295 the most important challenges in nanoscale devices is sensitivity to process variation, which can
 296 negatively impact the robustness of the circuits. It has been proven experimentally that the dominant
 297 source of variation in CNFET circuits is the nanotube density variations, which mainly results from
 298 variations in the spacing between CNTs on the substrate (*pitch*) and variations in the surviving CNT
 299 count after metallic CNT removal techniques [35]. Therefore, we used a Monte Carlo simulation to
 300 evaluate the CNT density variation with up to $\pm 15\%$ Gaussian distributions and variation at the $\pm 3\sigma$
 301 levels. As in Fig. 13, all the designs show robustness against CNT density variation.

302 In Table 6, delay, power and PDP of the ternary ALUs have been presented. In this table logic
 303 and arithmetic units' delays are presented separately. As we have predicted, delay and power
 304 consumption of the first ALU are slightly more than the second ALU. The PDP of the first ALU is
 305 about 19% more than the second one.

306 **Table 6.** Delay, power and Power Delay Product (pdp) of ternary ALUs

Design	Logic Delay (E-11s)	Arith Delay (E-11s)	Power (E-6W)	PDP (E-17J)
1 st ALU	2.175	6.699	13.11	87.82
2 nd ALU	1.652	6.307	11.68	73.66

307

308 5. Conclusion

309 In this paper, we present three output-states ternary logic circuits. Each of the presented circuits
 310 can perform a logic function or its complement via a control signal. When the circuits are idle *i.e.* not
 311 in use, the output is high impedance (HiZ), which lowers the power consumption. We design these
 312 circuits using carbon nano-tube field effect transistors (CNFETs). CNFETs are very appropriate for
 313 designing MVL circuits because of their ability to set the desired threshold voltage by adjusting the
 314 tubes' diameters. Moreover, two-digit adder/subtractor and two ternary ALUs have been designed
 315 using the proposed gates. The second ALU can reach the power efficiency by using the high
 316 impedance (HiZ) state of the gates when they are not in use. Circuits are simulated using HSPICE
 317 simulator with 32nm CNFET technology under different conditions. The results show robustness
 318 under process variation, temperature, and supply voltage. The AND/NAND gate has the lowest PDP
 319 compared to the other proposed designs because of its lower power dissipation. It has almost 48%
 320 lower PDP compared to the OR/NOR gate. Also by using the proposed designs in two-digit
 321 adder/subtractor, the power consumption is reduced more than 12X compared to the state-of-the-art
 322 designs.

323 **Acknowledgments:** The authors would like to thank the reviewers of their NANO'17 paper for their feedback
 324 which helped influence the presentation of this article. The authors would like to thank the members of the
 325 PEARL laboratory at New Mexico State University for the discussions and help.

326 References

- 327 1. A. Raychowdhury and K. Roy, "Carbon-nanotube-based voltage-mode multiple-valued logic design," *IEEE*
 328 *Transactions on Nanotechnology*, vol. 4, pp. 168-179, 2005.
- 329 2. E. Dubrova, "Multiple-valued logic in vlsi: Challenges and opportunities," in *Proceedings of NORCHIP*, 1999,
 330 pp. 340-350.
- 331 3. S. L. Hurst, "Multiple-valued logic—Its status and its future," *IEEE Transactions on Computers*, vol. 12, pp.
 332 1160-1179, 1984.
- 333 4. S. Tabrizchi, A. Panahi, F. Sharifi, K. Navi, and N. Bagherzadeh, "A novel method for designing ternary
 334 adder cell based on CNFETs," *IET Circuits, Devices & Systems*, 2017.
- 335 5. S. Lin, Y.-B. Kim, and F. Lombardi, "Design of a CNTFET-based SRAM cell by dual-chirality selection,"
 336 *IEEE Transactions on Nanotechnology*, vol. 9, pp. 30-37, 2010.
- 337 6. K. Roy, S. Mukhopadhyay, and H. Mahmoodi-Meimand, "Leakage current mechanisms and leakage
 338 reduction techniques in deep-submicrometer CMOS circuits," *Proceedings of the IEEE*, vol. 91, pp. 305-327,
 339 2003.

- 340 7. F. Sharifi, A. Panahi, H. Sharifi, K. Navi, N. Bagherzadeh, and H. Thapliyal, "Design of quaternary 4-2 and
341 5-2 compressors for nanotechnology," *Computers & Electrical Engineering*, vol. 56, pp. 64-74, 2016.
- 342 8. W. Porod, C. Lent, G. H. Bernstein, A. O. Orlov, I. Hamrani, G. L. Snider, *et al.*, "Quantum-dot cellular
343 automata: computing with coupled quantum dots," *International Journal of Electronics*, vol. 86, pp. 549-590,
344 1999.
- 345 9. G. Deng and C. Chen, "Binary multiplication using hybrid MOS and multi-gate single-electron transistors,"
346 *IEEE transactions on very large scale integration (VLSI) systems*, vol. 21, pp. 1573-1582, 2013.
- 347 10. Y.-B. Kim, "Challenges for nanoscale MOSFETs and emerging nanoelectronics," *Transactions on Electrical
348 and Electronic Materials*, vol. 11, pp. 93-105, 2010.
- 349 11. M. H. Moaiyeri, K. Navi, and O. Hashemipour, "Design and evaluation of CNFET-based quaternary
350 circuits," *Circuits, Systems, and Signal Processing*, vol. 31, pp. 1631-1652, 2012.
- 351 12. S. Lin, Y.-B. Kim, and F. Lombardi, "CNTFET-based design of ternary logic gates and arithmetic circuits,"
352 *IEEE transactions on nanotechnology*, vol. 10, pp. 217-225, 2011.
- 353 13. H. Mouftah and I. Jordan, "Implementation of 3-valued logic with cosmos integrated circuits," *Electronics
354 Letters*, vol. 10, pp. 441-442, 1974.
- 355 14. H. Mouftah and K. Smith, "Injected voltage low-power CMOS for 3-valued logic," in *IEE Proceedings G-
356 Electronic Circuits and Systems*, 1982, pp. 270-272.
- 357 15. R. C. G. da Silva, H. Boudinov, and L. Carro, "A novel voltage-mode CMOS quaternary logic design," *IEEE
358 Transactions on Electron devices*, vol. 53, pp. 1480-1483, 2006.
- 359 16. S. R. R. Datla and M. A. Thornton, "Quaternary voltage-mode logic cells and fixed-point multiplication
360 circuits," in *Multiple-Valued Logic (ISMVL), 2010 40th IEEE International Symposium on*, 2010, pp. 128-133.
- 361 17. A. Heung and H. Mouftah, "Depletion/enhancement CMOS for a lower power family of three-valued logic
362 circuits," *IEEE Journal of Solid-State Circuits*, vol. 20, pp. 609-616, 1985.
- 363 18. I. Thoidis, D. Soudris, I. Karafyllidis, S. Christoforidis, and A. Thanailakis, "Quaternary voltage-mode
364 CMOS circuits for multiple-valued logic," *IEE Proceedings-Circuits, Devices and Systems*, vol. 145, pp. 71-77,
365 1998.
- 366 19. V. P. KS and K. Gurumurthy, "Quaternary CMOS combinational logic circuits," in *Information and
367 Multimedia Technology, 2009. ICIMT'09. International Conference on*, 2009, pp. 538-542.
- 368 20. Y. Yasuda, Y. Tokuda, S. Zaima, K. Pak, T. Nakamura, and A. Yoshida, "Realization of quaternary logic
369 circuits by n-channel MOS devices," *IEEE Journal of Solid-State Circuits*, vol. 21, pp. 162-168, 1986.
- 370 21. J. Liang, L. Chen, J. Han, and F. Lombardi, "Design and evaluation of multiple valued logic gates using
371 pseudo N-type carbon nanotube FETs," *IEEE Transactions on Nanotechnology*, vol. 13, pp. 695-708, 2014.
- 372 22. S. Tabrizchi, F. Sharifi, Z. M. Saifulla, and A. H. Badawy, "Enabling Energy-Efficient Ternary Logic Gates
373 using CNFETs," in *17th IEEE International Conference on Nanotechnology, 2017*,
- 374 23. I. Amlani, A. O. Orlov, G. Toth, G. H. Bernstein, C. S. Lent, and G. L. Snider, "Digital logic gate using
375 quantum-dot cellular automata," *science*, vol. 284, pp. 289-291, 1999.
- 376 24. V. V. Zhirnov, J. A. Hutchby, G. Bourianoffls, and J. E. Brewer, "Emerging research logic devices," *IEEE
377 Circuits and Devices Magazine*, vol. 21, pp. 37-46, 2005.
- 378 25. J. Deng, "Device modeling and circuit performance evaluation for nanoscale devices: silicon technology
379 beyond 45 nm node and carbon nanotube field effect transistors," Stanford University, 2007.
- 380 26. Y. B. Kim, Y.-B. Kim, and F. Lombardi, "A novel design methodology to optimize the speed and power of
381 the CNTFET circuits," in *Circuits and Systems, 2009. MWSCAS'09. 52nd IEEE International Midwest
382 Symposium on*, 2009, pp. 1130-1133.
- 383 27. B. Wang, C.P. Poa, L. Wei, L.J. Li, Y. Yang and y. Chen, "(n, m) selectivity of single-walled carbon nanotubes
384 by different carbon precursors on Co-Mo catalysts" *Journal of the American Chemical Society*, vol. 129, pp.
385 9014-9019.
- 386 28. A. Lin, N. Patil, K. Roy, A. Badmaev, L.G. De Arco, C. Zhou, S. Mitra and H.-S.P. Wong, "Threshold voltage
387 and on-off ratio tuning for multiple-tube carbon nanotube FETs," *Nanotechnology, IEEE Transactions on*,
388 vol. 8, pp. 4-9, 2009.
- 389 29. H. Park, A. Afzali, S.-J. Han, G. S. Tulevski, A. D. Franklin, J. Tersoff, *et al.*, "High-density integration of
390 carbon nanotubes via chemical self-assembly," *Nature nanotechnology*, vol. 7, pp. 787-791, 2012.
- 391 30. N. Patil, J. Deng, H.-S. Wong, and S. Mitra, "Automated design of misaligned-carbon-nanotube-immune
392 circuits," in *Proceedings of the 44th annual Design Automation Conference*, 2007, pp. 958-961.

- 393 31. S. C. Kleene, N. de Bruijn, J. de Groot, and A. C. Zaanen, *Introduction to metamathematics* vol. 483: van
394 Nostrand New York, 1952.
- 395 32. M. H. Moaiyeri, A. Doostaregan, and K. Navi, "Design of energy-efficient and robust ternary circuits for
396 nanotechnology," *IET Circuits, Devices & Systems*, vol. 5, pp. 285-296, 2011.
- 397 33. J. Deng and H.-S. P. Wong, "A compact SPICE model for carbon-nanotube field-effect transistors including
398 nonidealities and its application—Part II: Full device model and circuit performance benchmarking," *IEEE*
399 *Transactions on Electron Devices*, vol. 54, pp. 3195-3205, 2007.
- 400 34. J. Deng and H.-S. P. Wong, "A compact SPICE model for carbon-nanotube field-effect transistors including
401 nonidealities and its application—Part I: Model of the intrinsic channel region," *IEEE Transactions on*
402 *Electron Devices*, vol. 54, pp. 3186-3194, 2007.
- 403 35. J. Zhang, N. Patil, H.-S. P. Wong, and S. Mitra, "Overcoming carbon nanotube variations through co-
404 optimized technology and circuit design," in *Electron Devices Meeting (IEDM), 2011 IEEE International*, 2011,
405 pp. 4.6. 1-4.6. 4.